Mathematical Modeling and Microbiological Verification of Ohmic Heating of a Multicomponent Mixture of Particles in a Continuous Flow Ohmic Heater System with Electric Field Parallel to Flow

Pitiya Kamonpatana, Hussein M. H. Mohamed, Mykola Shynkaryk, Brian Heskitt, Ahmed E. Yousef, and Sudhir K. Sastry

Abstract: To accomplish continuous flow ohmic heating of a low-acid food product, sufficient heat treatment needs to be delivered to the slowest-heating particle at the outlet of the holding section. This research was aimed at developing mathematical models for sterilization of a multicomponent food in a pilot-scale ohmic heater with electric-field-oriented parallel to the flow and validating microbial inactivation by inoculated particle methods. The model involved 2 sets of simulations, one for determination of fluid temperatures, and a second for evaluating the worst-case scenario. A residence time distribution study was conducted using radio frequency identification methodology to determine the residence time of the fastest-moving particle from a sample of at least 300 particles. Thermal verification of the mathematical model showed good agreement between calculated and experimental fluid temperatures ($P > 0.05$) at heater and holding tube exits, with a maximum error of 0.6 °C. To achieve a specified target lethal effect at the cold spot of the slowest-heating particle, the length of holding tube required was predicted to be 22 m for a 139.6 °C process temperature with volumetric flow rate of 1.0×10^{-4} m^3/s and 0.05 m in diameter. To verify the model, a microbiological validation test was conducted using at least 299 chicken-alginate particles inoculated with *Clostridium sporogenes* spores per run. The inoculated pack study indicated the absence of viable microorganisms at the target treatment and its presence for a subtarget treatment, thereby verifying model predictions.

Keywords: *Clostridium sporogenes*, mathematical model, multicomponent mixture, Ohmic heating, verification

Practical Application: The manuscript describes the detailed development and verification protocol of a mathematical model of a sterilization process for a liquid food containing 5 different types of solid food particles, within a continuous ohmic heater with electric field parallel to product flow. Our findings demonstrate that the model is capable of designing an ohmic thermal process for multicomponent solid–liquid food mixtures, and represents the development of a theoretical and experimental framework for companies interested in filing ohmic sterilization processes with the Food and Drug Administration.

Journal of Food Science A Publication of the Institute of Food Technologists

Introduction

The production of low-acid shelf-stable liquid foods containing particulates within continuous flow systems is of interest to the food industry (Sastry and Palaniappan 1992b; Zoltai and Swearingen 1996). Continuous flow ohmic heating has been considered to potentially avoid overheating and nutrient loss typical of conventional heat treatment. However, *in-situ* noninvasive temperature measurement of moving pieces in continuous flow is difficult, and limits our ability to assure product sterility in a straightforward manner. To address this problem, it is necessary to use mathematical models coupled with microbiological validation to ensure that the entire product is rendered commercially sterile.

Considerable literature now exists on modeling ohmic heating of solid–liquid mixtures. In static systems, models have been developed and experimentally verified: (including De Alwis and Fryer 1990, Sastry and Palaniappan 1992a, Fryer and others 1993, Sastry and Salengke 1998 and Salengke and Sastry 2007a,b). Models for solid–liquid mixtures in continuous flow systems have been developed by Sastry (1992), Zaror and others (1993), Sastry and Li (1996), Orangi and others (1998), and Chen and others (2010). Based on the literature, the potentially most dangerous situation occurs when the cold zone is within moving particles receiving insufficient heating. Therefore, it is necessary that mathematical models for continuous flow heating be verified by suitable protocols.

The microbiological validation protocols of a continuous aseptic process for particulate foods have been the subject of detailed development (Gaze and Brown 1990; Cacace and others 1994;

MS 20130884 Submitted 6/28/2013, Accepted 9/18/2013. *Author Kamonpatana is with Dept. of Food Science and Technology, Kasetsart Univ., Thailand. Author Mohamed is with Dept. of Food Hygiene and Control, Cairo Univ., Egypt. Authors Shynkaryk and Heskitt are with Dept. of Food, Agricultural and Biological Engineering, The Ohio State Univ., U.S.A. Author Yousef is with Dept. of Food Science and Technology, The Ohio State Univ., U.S.A. Author Sastry is with Dept. of Food, Agricultural and Biological Engineering, The Ohio State Univ., U.S.A. Direct inquires to author Sastry (E-mail: sastry.2@osu.edu).*

doi: 10.1111/1750-3841.12287

Naim and others 2008) and discussion. Protocols for verification are described by Marcy (1997), using model food/alginate particles inoculated with a known thermally resistant surrogate. It is necessary to study a sufficiently large number of samples (299) to ensure that at least 1 scenario involving a fast-moving particle in the 99th percentile is sampled (Digeronimo and others 1997).

We have recently reported on a study wherein modeling and verification were conducted for a product with a single-particle type (water chestnut), within a heater wherein the electric field is perpendicular to the product flow (Kamonpatana and others 2013). However, little work exists on the modeling and verification protocols for liquids containing many different particle types, and systems with electric field parallel to product flow (Chen and others 2010 describe a sensitivity analysis but do not provide details of the validation protocol). Accordingly, our objectives were to develop a mathematical model for the sterilization of a multicomponent solid–liquid food mixture within a continuous flow ohmic heater with electric field parallel to the product flow; and to thermally, electrically and microbiologically verify model predictions of a safe sterilization process within a pilot-scale system.

Materials and Methods

Product

The product chosen was chicken chow mein; used as a ration by the U.S. military. The formulation composed of 28.00% w/w of frozen 0.021 m cubic cooked chicken pieces of boneless skinless chicken breast, 14.13% w/w of cut celery (0.013 m), 6.00% w/w of cut mushrooms (0.013 m), 7.00% w/w of bean sprouts, and 6.00% w/w of canned sliced water chestnuts (0.01 m) in chow mein sauce. Details of product formulation and preparation for the ohmic process have been provided by Sarang and others (2007).

Product preparation

Prior to processing the product through the continuous flow ohmic heating system, various components were pretreated in accordance with protocols determined from prior experimentation to yield electrical conductivities that were as closely matched as possible. Cut mushroom, bean sprouts, canned sliced water chestnut, and cut celery were blanched in prepreparation blanching sauce for 6 min, 10 s, 1.5 min, and 8 min, respectively, at 100 °C. Chicken pieces were marinated for 1 h and 40 min in the sauce (pH 6.1) at room temperature. The formulation of chow mein sauce and prepreparation blanching sauce is described by Sarang and others (2007). More details regarding pretreatment are presented later in this manuscript.

Ohmic heating pilot plant

The product was processed in a 54 kW ohmic heating pilot plant (Figure 1A) located at The Ohio State Univ. The system consisted of 3 independent ohmic heaters with agitators and electric field parallel to the flow (Figure 1B). The pilot plant was composed of a 190 L mixing tank with a variable speed mixer model IIII/2-100 (Dover Corporation, Downers Grove, Ill., U.S.A.), a positive displacement pump (Moyno, Inc., Springfield, Ohio, U.S.A.), a magnetic flow meter (Rosemount Inc., Chanhassen, Minn., U.S.A.), three ohmic heaters, a holding tube, a scraped surface heat exchanger (Waukesha Cherry-Burrell, Delavan, Wis., U.S.A.) for primary cooling, a tubular heat exchanger (Waukesha Cherry-Burrell) for secondary cooling, an aseptic tank, and a laminar flow hood with high-efficiency particulate air (HEPA)-filtered air. Temperature of the chow mein sauce at the center of the cross-section of the exit of heating and holding sections was continuously measured with type-T thermocouples and recorded every 4 s using an Agilent 34970A data acquisition unit (Agilent Technologies, Inc., Palo Alto, Calif., U.S.A.). The voltage and current were monitored with Wonderware InTouch software Version 9.5 (Invensys Systems, Inc., Foxboro, Mass., U.S.A.).

Overall work

Our approach involves the use of conservative, yet reasonable assumptions in all cases. Details of worst-case considerations have been presented by Kamonpatana and others (2013) in relation to an electric field perpendicular to the flow, and will not be repeated here. In theory, the worst case involves a particle of properties widely differing from its immediate surroundings, in particular a completely nonconductive particle. To design the worst case around such a particle would sacrifice the advantage of ohmic heating, creating exceptionally long holding tubes and overprocessed product. Thus, we considered the worst case to correspond to a particle that was lower than 2 standard deviations below the lowest conductivity particle, adding additional factors of safety in the model, including relatively large size, low residence time, and slow heat transfer characteristics.

The basic procedures were as follows:

1. Determination of electrical conductivity, specific heat, thermal conductivity, and density of chow mein sauce, all particulate components and surrogate chicken-alginate particles. Also, all particle dimensions were measured.
2. Formulation of chicken-alginate particles as conservative surrogates for the slowest-heating particle, for use in residence time distribution (RTD) and microbiological studies.
3. Determination of RTD of moving particles to determine the fastest-moving particle in the system.
4. Determination of thermal inactivation kinetics of *Clostridium sporogenes* ATCC 7955 (PA 3679) spores in chicken-alginate particles to use in modeling, and to verify that the *Z*-value was the same as that presumed for *C. botulinum*.
5. Development of mathematical model based on a two-part simulation approach (Sastry and Cornelius 2002):
   a. Fluid temperature simulation (Sastry 1992) to compute fluid temperature through the heater and an arbitrarily long hold-tube section, the average temperature of solid particles and the current drawn by the system.
   b. Worst-case scenario using the residence time of the fastest-moving particle from the RTD study, the kinetic data on the test microorganism, and the fluid temperatures determined in the simulations above, to compute the required size of the holding tube.
6. Thermal and electrical verification of the model by comparing predicted and experimental temperatures of the liquid phase at the exit of heating and holding sections; and calculated and experimental values of current in the three ohmic heating sections.
7. Microbiological validation of the model using chicken-alginate particles inoculated with *C. sporogenes* spores that were recovered and cultured to determine if survivors existed postprocessing.

Properties of chicken chow mein components

Density of chow mein sauce and particles was determined by the weight/volume method using a 0.001 m^3 graduated glass cylinder (Fisher Scientific, Pittsburgh, Pa., U.S.A.) (Shynkaryk and Sastry 2012).

Specific heat of all components was determined by a differential scanning calorimeter (model 2920 modulated DSC, TA Instruments, New Castle, Del., U.S.A.) (King and Kaletunc 2009).

Thermal conductivities were determined from composition data (USDA Handbook 8, USDA 2011, online) using the equations given by Singh and Heldman (2001). To represent a realistic temperature during processing, all values were calculated at a temperature of 100 °C, since the thermal conductivity at this temperature was lower than at the maximum temperature, yielding a reasonably conservative value over the temperature range 80–140 °C.

The electrical conductivity of each component (10 samples each) was determined using the methodology of Sarang and others (2008).

Unless otherwise specified, each experiment was carried out at least in triplicate.

Formulation of chicken-alginate particles

Although the electrical conductivity of the chicken particles was found to be lowest (data shown later), we needed to consider that particles other than chicken might have been the slowest heating. Screening simulations for each of the other particle types, using residence times within the heating section that were 0.8 times that

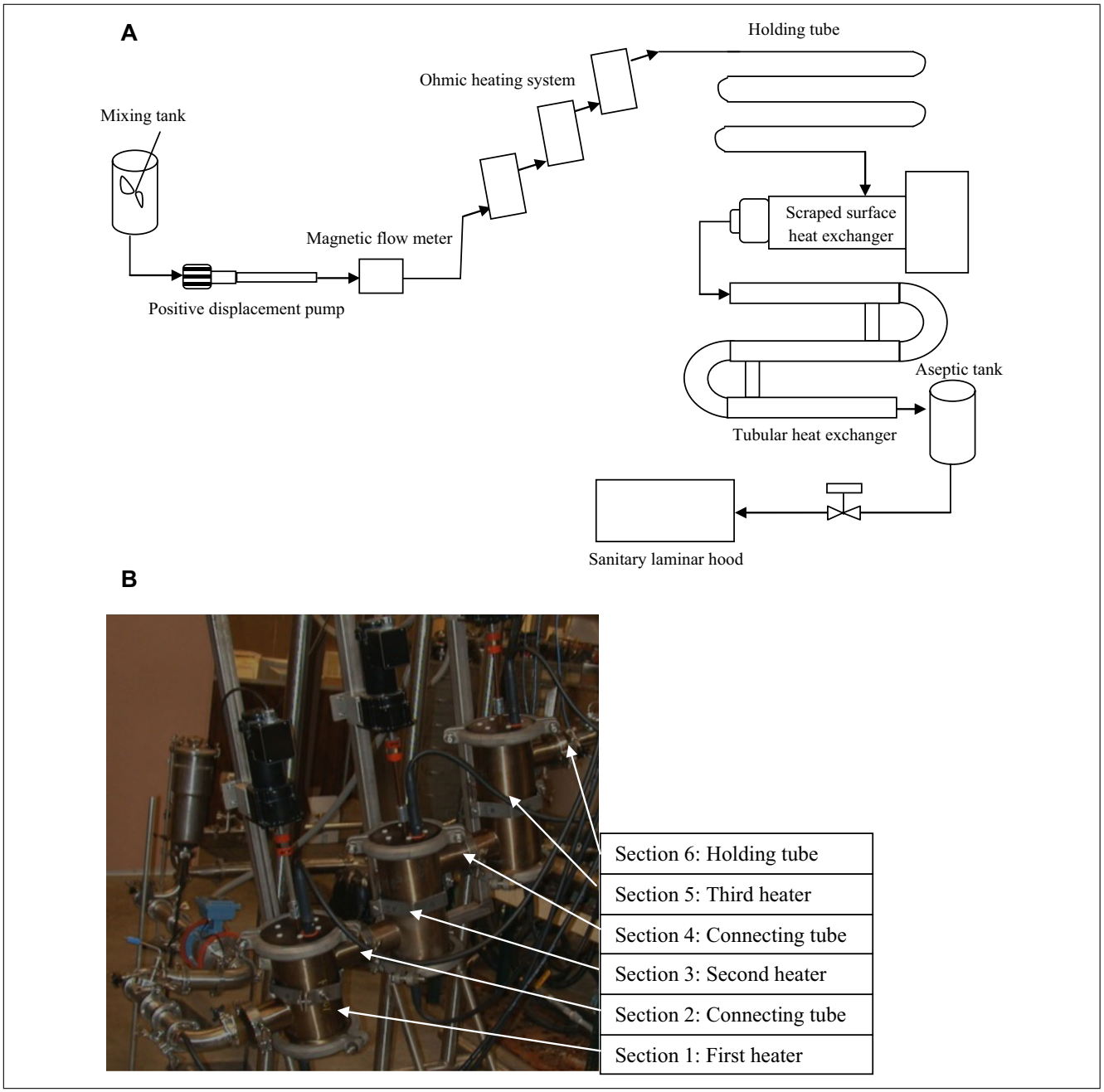

Figure 1–(A) A schematic diagram of a continuous flow ohmic heating process and (B) three ohmic heaters with product flow parallel to electric field.

Table 1–Chicken-alginate analog formulation.

Ingredient	Percent by weight
Strained chicken baby food	91.47
Calcium sulfate	0.38
Tri-sodium citrate	0.08
Yeast extract	0.10
Glucose	0.10
$FeSO_4 \cdot 7H_2O$	0.03
Salt	3.92
Sodium alginate	3.92
Green colored food dye	

of the fastest-chicken particles (data for chicken residence times shown later) indicated that even under such situations, holding tubes sized based on the chicken particle were the longest. Thus, we formulated chicken-alginate particles to represent the worst case, for use in the RTD study and serve as surrogates for microbiological validation. The particles were of cubes (0.021 m × 0.021 m × 0.021 m). The formulation (Table 1) was finalized based on results of several trials to simulate the worst case with average electrical conductivity and thermal diffusivity values less than those of the slowest-heating particle. Formulation techniques were modified from those of Brown and others (1984). Preparation steps are detailed below:

Baby foods (chicken and chicken broth, Beech-Nut Nutrition Corp, N.Y., U.S.A.) and ingredients listed in Table 1, except sodium alginate, were homogenized in a blender (3 min). A colored food dye (The Kroger Co., Columbus, Ohio, U.S.A.) was added to identify these particles for recovery postprocessing. The puree was transferred to containers and sterilized in an autoclave for 30 min at 121 °C, taking special care to minimize contamination risk. The autoclaved puree was poured to a sterile blender. A spore suspension of *C. sporogenes* PA 3679 was added, followed by sterile sodium alginate. The mixture was rapidly stirred for 5 min, shaped into a 0.021 m slab and immersed in 2% w/v sterile calcium chloride solution for 17.5 h at 4 °C. The slabs were formed into a cubical shape, and left in 2% w/v sterile calcium chloride solution for 3.5 h at 4 °C. The particles were drained and kept at 4 °C before use. The finished particles contained approximately 5.6×10^5 CFU/g. For the RTD study, the inoculation step was omitted.

Kinetic parameters of *C. sporogenes* spores

Thermal inactivation kinetics of *C. sporogenes* spores in chicken-alginate puree matrix were investigated to test whether the temperature sensitivity (*Z*-value) was the same as the presumed value (10 °C) of *C. botulinum*. Tests were conducted at 118, 123, and 130 °C using custom-fabricated aluminum tubes (11 mm internal diameter and 37.8 mm long), using a procedure modified from Rajan and others (2006). Procedures are as described by Kamonpatana and others (2013) except that the heating times (recorded when the temperature reached the target temperature) were 0, 2, 4, and 8 min at 118 °C; 0, 20, 40, and 60 s at 123.0 °C; and 0, 5, 10, and 15 s at 130 °C.

RTD study

The fastest particle residence time in the heating and holding sections was determined from a RTD study using the radio frequency identification (RFID) methodology described by Tulsiyan and others (2009) and Sarang and others (2009). RFID readers (TRRO1OEM, Intersoft Corp., Tullahoma, Tenn., U.S.A.) with circular antennae (Intersoft Corp.) were installed (Figure 2A): at the heater inlet, the heater outlet, and the holding tube outlet. Over 299 chicken-alginate particles imbedded with RFID tags (Figure 2B) were added to the chicken chow mein, mixed and processed through the system. The signals of RFID tags were read and recorded when the tags passed through the readers. The difference in time of a tracer between 2 readers was the residence time of each tracer. The product mean residence time (t_m) was obtained from

$$t_m = \frac{\rho V}{\dot{m}} \quad (1)$$

The normalized times were the ratio of the empirical particle residence times to the product mean residence time. The minimum normalized particle residence time (MNPRT) was applied in the mathematical model for the worst-case scenario simulations.

Mathematical modeling

The mathematical model involved solution of interdependent thermal and electrical problems (Sastry and Palaniappan 1992a). Two simulations were conducted: fluid temperature prediction and worst-case scenario, as discussed at the NCFST-CAPPS Workshops on Aseptic Processing of Multiphase Foods (Sastry 1997), and described in greater detail by Sastry and Cornelius (2002) for aseptic processing involving conventional heat exchangers. The modeling and simulation were developed with a FORTRAN 90 program and run in the Ohio Supercomputer Center's IBM Cluster 1350.

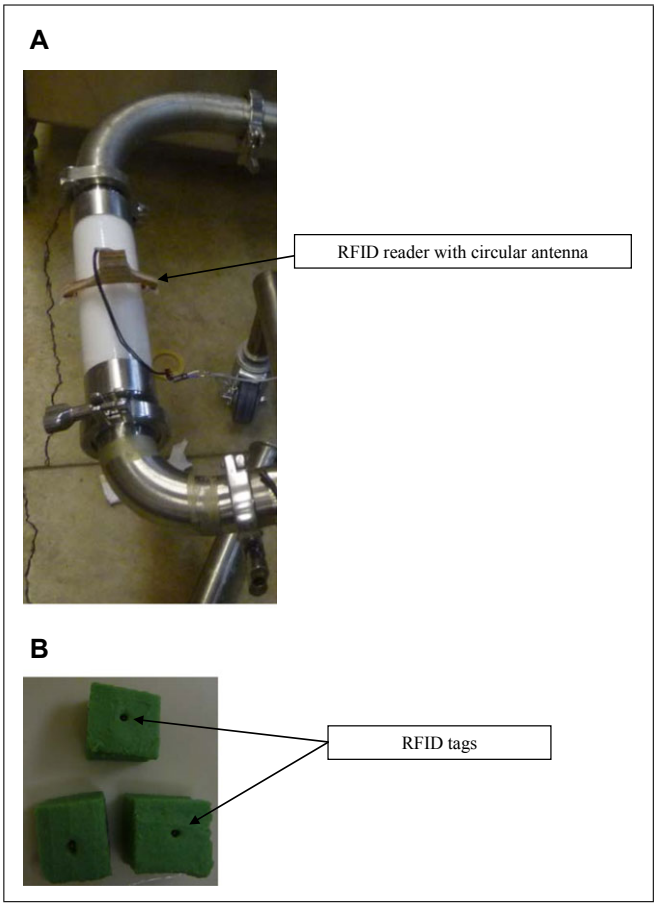

Figure 2–(A) RFID reader with circular antenna and (B) tags.

a Fluid temperature simulation

Fluid and solid pieces were assumed to move under plug flow (fluid and solid moving at the same velocity) through heating and holding sections. This assumption is generally reasonable for high solid concentration: it allows calculation of fluid temperatures through the length of the heater and holding sections, and permits the evaluation of worst-case scenarios as special cases. For a liquid containing 5 different types of solid particles, the differential equation for the energy balance may be cast as

$$\frac{\dot{m}_f C_{pf}}{A_{cs}} \frac{dT_f}{dx} = \dot{u}_f - \sum_{i=1}^{5} n_i h_i a_i \left(T_f - T_i\right) - U a_w \left(T_f - T_a\right) \tag{2a}$$

where the index i represents a given particle type. Within an increment(Δx), between locations n and $n+1$, the energy balance on the well-mixed liquid phase may be written as

$$\begin{aligned} &\dot{m}_f C_{pf}(T_f^{n+1} - T_f^n) = \dot{u}_f v_f - n_{chk} h_{chk} A_{chk}(T_f^m - T_{chk}^m) \\ &- n_{clr} h_{clr} A_{clr}(T_f^m - T_{clr}^m) - n_{mr} h_{mr} A_{mr}(T_f^m - T_{mr}^m) \\ &- n_{bn} h_{bn} A_{bn}(T_f^m - T_{bn}^m) - n_{chn} h_{chn} A_{chn}(T_f^m - T_{chn}^m) \\ &- U A_w(T_f^m - T_a) \end{aligned} \tag{2b}$$

where

$$T_{chk}^m = \frac{T_{chk}^{n+1} + T_{chk}^n}{2} \tag{3}$$

$$T_{clr}^m = \frac{T_{clr}^{n+1} + T_{clr}^n}{2} \tag{4}$$

$$T_{mr}^m = \frac{T_{mr}^{n+1} + T_{mr}^n}{2} \tag{5}$$

$$T_{bn}^m = \frac{T_{bn}^{n+1} + T_{bn}^n}{2} \tag{6}$$

$$T_{chn}^m = \frac{T_{chn}^{n+1} + T_{chn}^n}{2} \tag{7}$$

$$T_f^m = \frac{T_f^{n+1} + T_f^n}{2} \tag{8}$$

v_f is the liquid volume in the incremental section:

$$v_f = \frac{\pi}{4}(D^2 - d^2)\Delta x \phi_f \tag{9}$$

and the rate of energy generation of liquid is

$$\dot{u}_f = |\nabla V|^2 \sigma_{0f}(1 + m_f T_f^m) \tag{10}$$

Internal temperature of the solid pieces may be determined by using the transient 3 dimensional heat conduction equation:

$$\rho_s C_{Ps} \frac{\partial T_s}{\partial t} = \nabla \bullet (k_s \nabla T_s) + \dot{u}_s \tag{11}$$

where the rate of energy generation term ($\dot{u}_s$) in Eq. (11) is given by

$$\dot{u}_s = |\nabla V|^2 \sigma_{0s}(1 + m_s T_s) \tag{12}$$

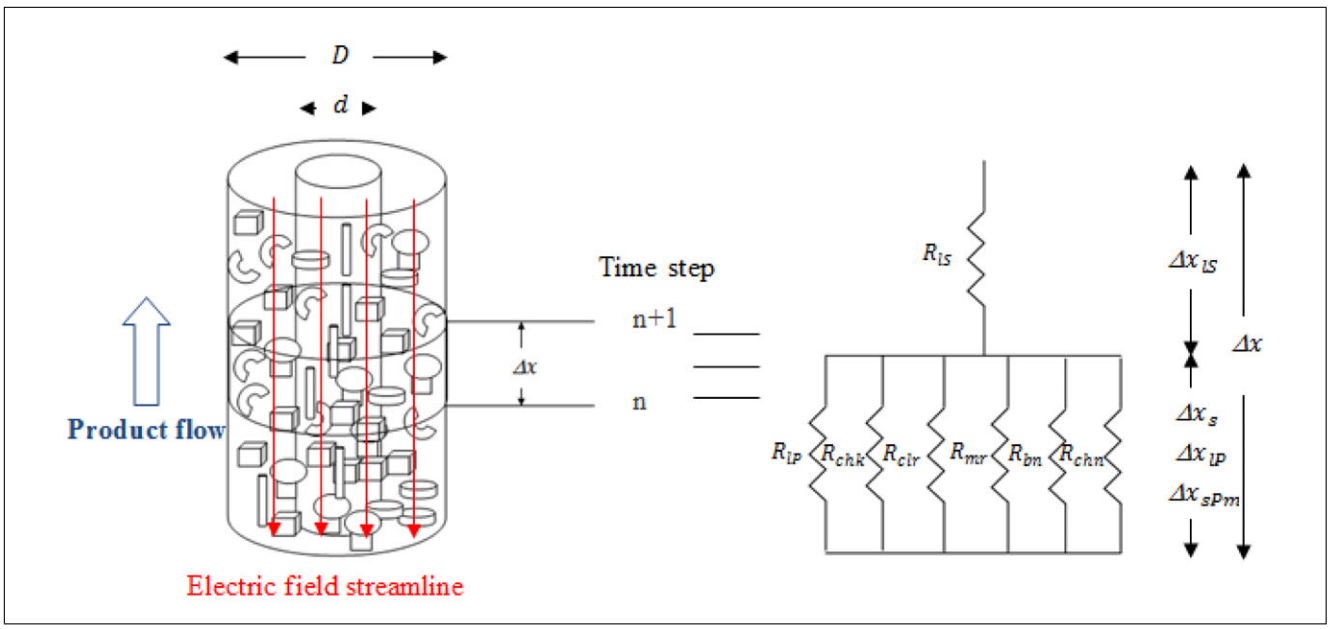

Figure 3–Equivalent circuit of a multicomponent mixture.

Table 2–Experimental system parameters used in the program (see Figure 1B for section details).

Section	Diameter (D) (m)	Shaft diameter (d) (m)	Length (m)	Initial temperature (°C)	Voltage at target (V)	Voltage under target (V)	h_{fp} (W/m^2 °C)	U (W/m^2 °C)
1	0.14	0.05	0.15	81.0	117	99	200	1
2	0.05	0.00	0.18	–	–	–	200	1
3	0.14	0.05	0.20	–	117	99	200	1
4	0.05	0.00	0.18	–	–	–	200	1
5	0.14	0.05	0.25	–	117	99	200	1
6	0.05	0.00	22.00	–	–	–	200	10

–Not applicable.

Table 3–Properties of chicken chow mein product and chicken-alginate particle.

	Percent by weight	Treatment	Thickness m	Specific heat J/kg °C	Thermal conductivity W/m °C	Density kg/m^3	Diffusivity m^2/s	σ_0[d] S/m	m[d] 1/°C
Chow mein sauce	38.87	–	–	3917.99	0.60	1019.08[a,c]	–	1.78	0.05
Boneless skinless chicken breast (slowest heating particle)	28.00	Marinating 1.67 h	0.021	3402.10[a]	0.57	1081.80[b]	1.55×10^{-7}	2.00	0.02
Celery	14.13	Blanching 8 min	0.013	3953.36	0.66	1053.79[a,b]	1.58×10^{-7}	1.90	0.02
Mushroom	6.00	Blanching 6 min	0.013	3683.55	0.63	1076.27[b]	1.59×10^{-7}	0.62	0.08
Bean sprout	7.00	Blanching 10 s	–	4015.41	0.64	1004.32[c]	1.59×10^{-7}	1.09	0.04
Water chestnut	6.00	Blanching 1.5 min	0.010	3784.42	0.65	1055.8[b]	1.63×10^{-7}	0.46	0.12
Chicken-alginate particle	–	–	0.021	3692.72[b]	0.55	1060.60[b]	1.40×10^{-7}	1.39	0.03
Chicken-alginate particle with RFID tag	–	–	0.021	–	–	1069.40[b]	–	–	–

[a–c]Mean values of density and specific heat sharing the same superscript are not significantly different ($P > 0.05$).
[d]σ_0 and m were applied in Eq. (10) to calculate the rate of energy generation for liquid and Eq. (12) for solid particle.
–Not applicable.

Equation (11) has a time-dependent convective boundary condition[1]

$$-k_s \nabla T_s \bullet \vec{n} = h_{fp}\left(T_s - T_f(t)\right) \tag{13}$$

at all external surfaces. Computational effort was reduced using symmetry considerations: the symmetry surface was considered as no heat flux (insulated boundary):

$$\nabla T_s \bullet \vec{n} = 0 \tag{14}$$

at all symmetry surfaces.

Electric field distribution. The effective electrical resistance can be determined by an extension to multicomponent mixtures (schematic in Figure 3), of the approach of Palaniappan and Sastry (1991), Sastry (1992), and Sastry and Palaniappan (1992a,b)

$$R_n = R_{lS} + R_P \tag{15}$$

$$R_p = \frac{1}{\frac{1}{R_{lP}} + \sum_{m=1}^{5} \frac{1}{R_{sPm}}}$$

$$R_p = \frac{1}{\frac{1}{R_{lP}} + \frac{1}{R_{chk}} + \frac{1}{R_{clr}} + \frac{1}{R_{mr}} + \frac{1}{R_{bn}} + \frac{1}{R_{chn}}} \tag{16}$$

[1]It may be argued that the use of heat transfer coefficients is outdated, and that a heat flux continuity boundary condition should be used. In our view, this is not possible, because it would require knowledge of the entire flow field surrounding all particles in a multiphase system with irregular and differing particle shapes. Although particle mover codes may be used to track this problem for spherical particles to some extent, a comprehensive simulation of all possible particle scenarios for a product as complex as chicken chow mein is not yet on the horizon.

where

$$R_{lS} = \frac{\Delta x_{lS}}{A_{lS}\sigma_l} \tag{17}$$

$$R_{lP} = \frac{\Delta x_{lP}}{A_{lP}\sigma_l} \tag{18}$$

$$R_{sPm} = \frac{\Delta x_{sPm}}{A_{sPm}\sigma_{sm}} \tag{19}$$

The length of the incremental section is the sum of the length of solid and liquid phases:

$$\Delta x = \Delta x_{lS} + \Delta x_{lP} \tag{20}$$

where

$$\Delta x_{sPm} = \Delta x_{lP} \tag{21}$$

Area of liquid phase in series (A_{lS}) is equivalent to the area of cross section of the heater($A = \frac{\pi}{4}(D^2 - d^2)$), and equal to the area of liquid and solid phases connected in parallel:

$$A_{lS} = A_{lP} + A_{sP} = A_{lP} + \sum_{m=1}^{5} A_{sPm} \tag{22}$$

Based on the model described originally by Kopelman (Palaniappan and Sastry 1991; Sastry 1992; Sastry and Palaniappan 1992b), the effective length and area of the solid phase could

be calculated from its volume fraction (ϕ_s) as

$$\Delta x_s = \Delta x_{s\,Pm} = \Delta x \phi_s^{\frac{1}{3}} \tag{23}$$

and:

$$A_{s\,P} = \sum_{m=1}^{5} A_{s\,Pm} = A\phi_s^{\frac{2}{3}} \tag{24}$$

From the above set of relations, the lengths of the liquid phase in series and parallel are

$$\Delta x_{l\,S} = \Delta x(1 - \phi_s^{\frac{1}{3}}) \tag{25}$$

$$\Delta x_{l\,P} = \Delta x \phi_s^{\frac{1}{3}} \tag{26}$$

and the areas of liquid phase in the series and parallel regions are

$$A_{l\,S} = A \tag{27}$$

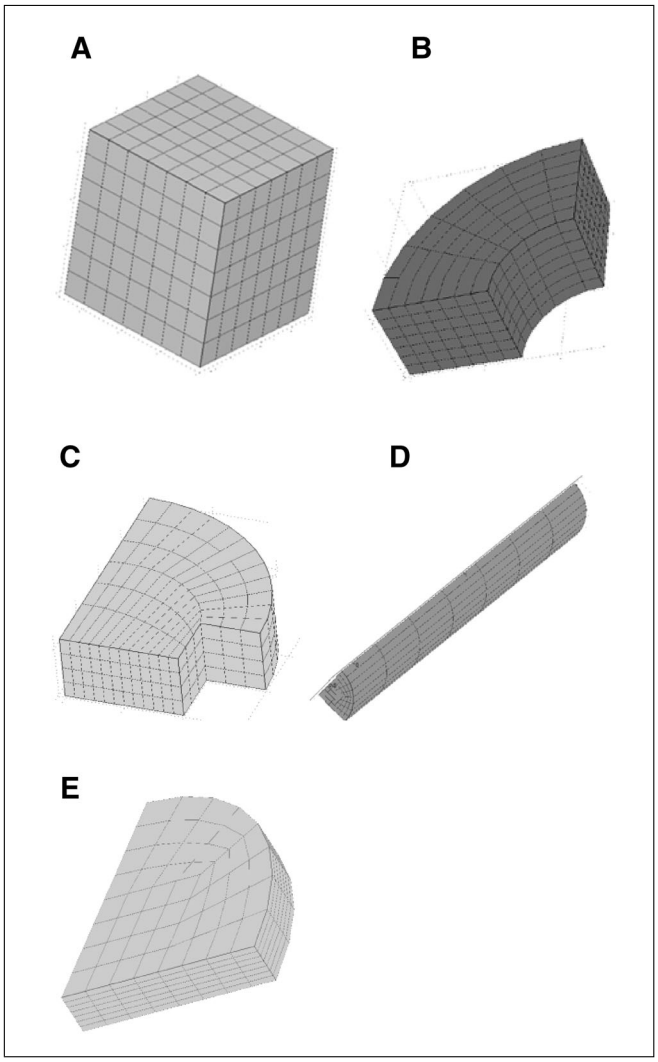

Figure 4–Finite-element grid of (A) chicken pieces, (B) cut celery, (C) cut mushroom, (D) bean sprouts, and (E) sliced water chestnut.

and

$$A_{l\,P} = A(1 - \phi_s^{\frac{2}{3}}) \tag{28}$$

The volume of each individual solid phase ($v_{s\,m}$) is the product of its fraction ($\phi_{s\,m}$) cross-sectional area and the length of the incremental section:

$$v_{s\,m} = A\phi_{s\,m}\Delta x \tag{29}$$

The area of each individual particle phase, the ratio of its volume ($v_{s\,m}$) to length ($\Delta x_{s\,Pm}$), is given by

$$A_{s\,Pm} = \frac{A\phi_{s\,m}}{\phi_s^{\frac{1}{3}}} \tag{30}$$

The total resistance of the heating section is then

$$R = \sum_{n=1}^{N} R_n \tag{31}$$

The current drawn within each heating section is the applied voltage divided by the total resistance (R).

$$I = \frac{V}{R} \tag{32}$$

The field strength (voltage gradient) may be calculated for each incremental step as

$$\nabla V_n = \frac{I R_n}{\Delta x} \tag{33}$$

Solution Procedure. Simulations were conducted using the experimental system parameters given in Table 2. The value of the overall heat transfer coefficient (U) between product and external environment was determined experimentally from Eq. (2) without particle terms, using the data on heating of sodium sulfate solution during presterilization for each trial. U values determined in heating and holding sections are shown in Table 2. Product properties are presented in Table 3. Mesh refinement simulations were conducted (not shown) for optimization.

Three major equations, Eq. (2), (11), and (33), were simultaneously solved and updated to determine fluid temperature, particle temperature, and electric field strength in the following manner. T_f^1, T_{chk}^1, T_{clr}^1, T_{mr}^1, T_{bn}^1, and T_{chn}^1 at the 1st time step were specified as initial temperature shown in Table 2. The fluid temperature (T_f^n) of each time step was calculated by using Eq. (2) and applied as the surface temperature of the solid ($T_f(t)$) in Eq. (13). The heat conduction equation for Eq. (11) satisfying boundary conditions Eq. (13) and Eq. (14) could be solved to determine temperature distribution within each particle type by using the finite-element procedures detailed (and experimentally verified) by Sastry and Palaniappan (1992a). For this purpose, grids were generated for each particle type within the domain (Figure 4). T_{chk}^{n+1}, T_{clr}^{n+1}, T_{mr}^{n+1}, T_{bn}^{n+1}, and T_{chn}^{n+1} were assumed to be equal to T_{chk}^n, T_{clr}^n, T_{mr}^n, T_{bn}^n, and T_{chn}^n for the 1st iteration of Eq. (2), which was applied to compute the fluid temperature for the next step (T_f^{n+1}). The field strength for each time step (∇V_n) depends on current and resistance, which is influenced by temperature, and was calculated in Eq. (33). Then, T_{chk}^{n+1}, T_{clr}^{n+1}, T_{mr}^{n+1}, T_{bn}^{n+1}, and T_{chn}^{n+1}

were derived from Eq. (11) by using the above updated value of $T_f(t)$ in Eq. (13) and ∇V in Eq. (12); and subsequently used as an updated T_f^{n+1} for the next iteration of Eq. (2). This entire procedure was repeated till convergence with a relative error of 0.0001%.

b. Worst-case simulation

Once the fluid temperature is determined, it is possible to conduct worst-case simulations related to unusual (inclusion) particles, for example, with unusual electrical conductivity, residence time, or other properties. The worst-case particle was assumed to have

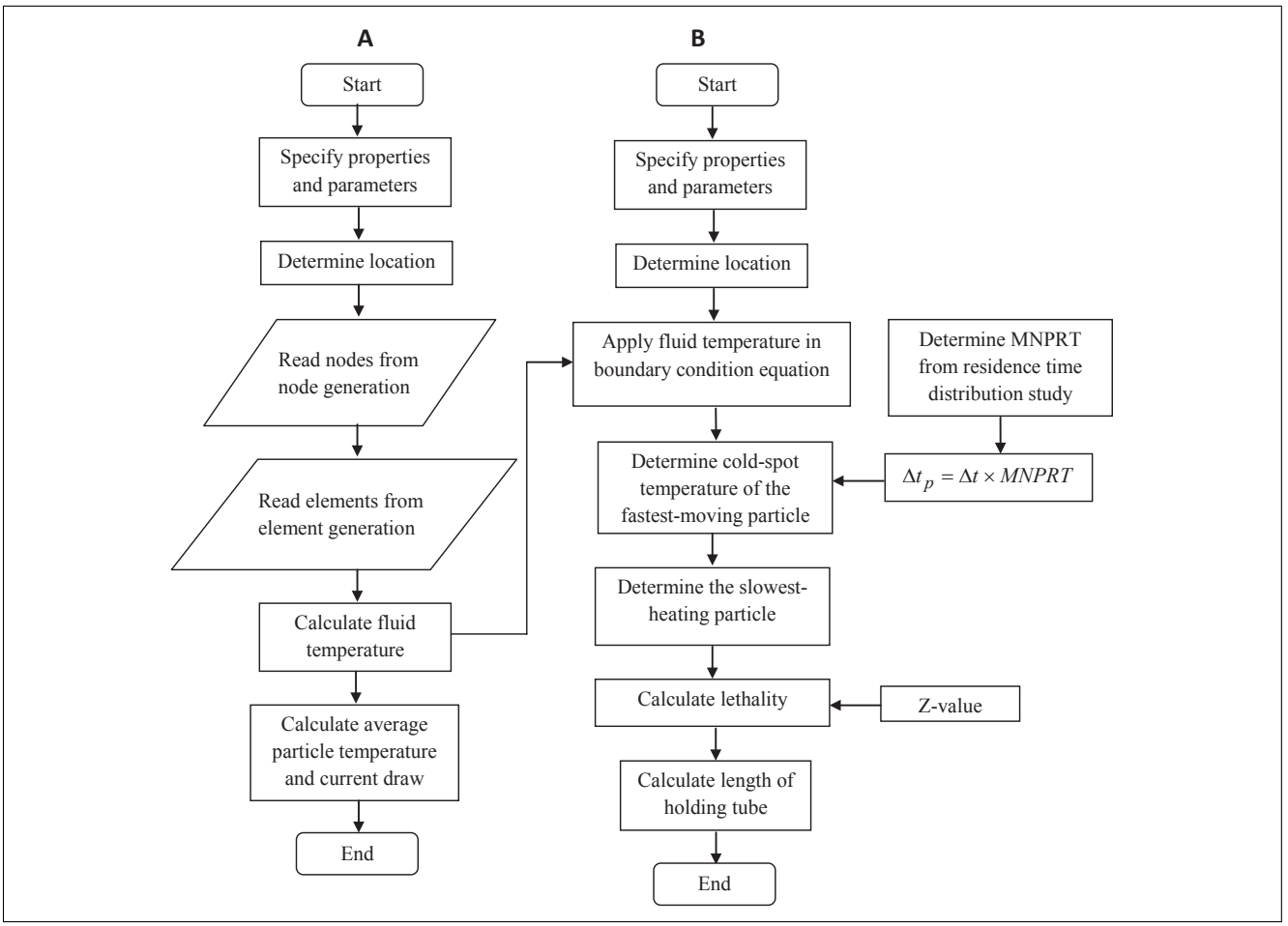

Figure 5–Program flowchart showing (A) fluid temperature simulation and (B) worst-case simulation.

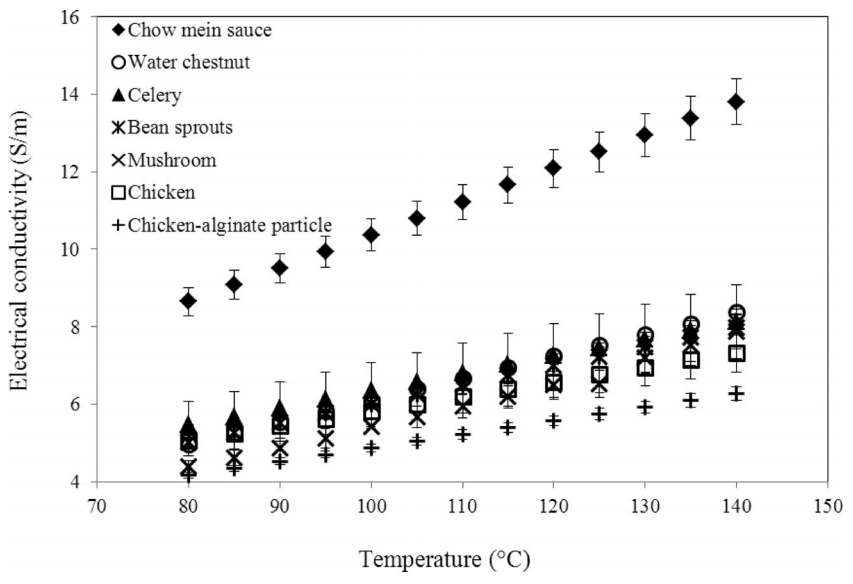

Figure 6–Electrical conductivity of chicken chow mein composition and chicken-alginate particle (mean ± 2S.D) compared with temperature at 60 Hz.

Table 4–Decimal reduction times (*D*-values) and *Z*-value of *C. sporogenes* PA 3679 spores in chicken-alginate puree treated with conventional heating.

Temperature (°C)	*D*-values (minute)	R^2	*Z*-value (°C) (R^2)
118.0	1.94	0.99	10 (0.94)
123.0	0.28	0.95	
130.0	0.09	0.96	

characteristics similar to chicken-alginate particles that were carefully formulated to represent conservative properties. The electrical conductivity of the chicken-alginate particles was more than 2 standard deviations below that of the lowest electrical conductivity particle (data shown under Results and Discussion section). Size and density were not significantly different from those of the slowest-heating particle (Table 3). Specific heat was higher, while thermal conductivity was lower than the slowest-heating particle (Table 3). The h_{fp} value was computed based on the size of the biggest particle (chicken cubes) and the equation from Ranz and Marshall (1952). For a flow behavior index of 0.29 (Shynkaryk and Sastry 2012) and the minimum relative velocity between fluid and particle of 0.02 m/s (Balasubramaniam and Sastry 1994), the h_{fp} value was found to be 230 W/m^2 °C at 80 °C. This relation was obtained from a study of spherical particles, for which the h_{fp} value was not different from that of cubic shapes with the same volume (Astrom and Bark 1994). For conservatism, the value was chosen at 200 W/m^2 °C (Table 2), considered to be conservative, but reasonable, given that the fastest-moving particle would more than likely have a greater relative velocity than that measured by Balasubramaniam and Sastry (1994) and Zitoun and others (2001). The actual value of h_{fp} resulted in a small effect on fluid temperature predictions; therefore, h_{fp} of 200 W/m^2 °C was chosen for all sections of the system. The temperature of the solid particle was calculated using Eq. (11) the same as for fluid temperature simulations. The fluid temperatures (T_f^n) of each time step from fluid temperature simulations were imported into the worst-case simulation and set as boundary conditions for solid particles in Eq. (13). The program simultaneously computed 5 different types of solid particles including the chicken-alginate particles. The values of Δx remained unchanged from fluid temperature simulation. However, due to a presumed higher particle speed, the incremental time of the particle (Δt_p) was smaller than Δt implying that the particle experienced the existing environmental conditions at an accelerated rate (Sastry and Cornelius 2002):

$$\Delta t_p = \Delta t \times \text{MNPRT} \tag{34}$$

The accumulated lethality (F_0) of the cold spot of the slowest-heating particle can be expressed as (Sastry and Cornelius 2002)

$$F_0 = \int_0^{t_h} 10^{\frac{T_c(t)-T_{ref}}{Z}} dt \cong \sum_0^{t_h} \Delta t_p 10^{\frac{T_c(t)-T_{ref}}{Z}} \tag{35}$$

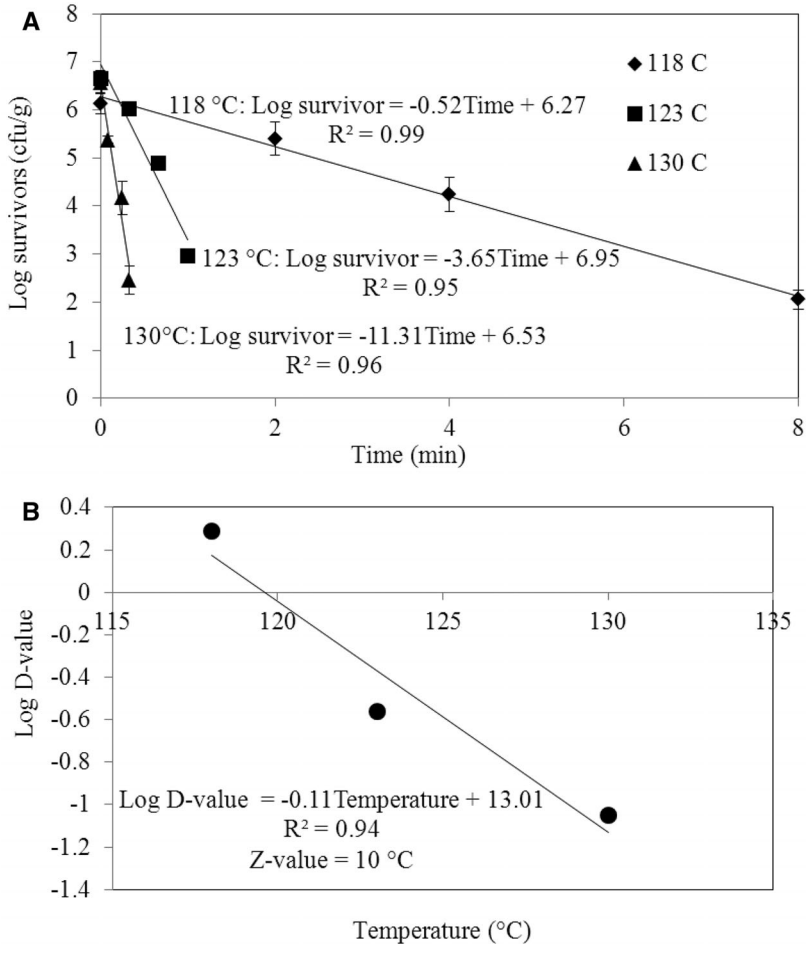

Figure 7–(A) Inactivation of *C. sporogenes* PA 3679 spores in chicken-alginate puree under conventional heating at different temperatures and (B) thermal death time curve (Log *D*-value compared with temperature) of *C. sporogenes* PA 3679 spores in chicken-alginate puree.

Table 5–Experimental residence time data of the ohmic heater and holding section.

	Number of tracers	Residence time	Minimum tracer residence time	Mean tracer residence time	Maximum tracer residence time
Heating section	344	Measured (s)	76	105	228
		Normalized	0.64	0.89	1.93
Holding section	442	Measured (s)	362	376	486
		Normalized	0.84	0.87	1.13

where the reference temperature (T_{ref}) is 121.1 °C and the Z-value is as determined previously in Kinetic parameters of *C. sporogenes* spores section.

The holding tube length was calculated by computing the accumulated F_0 incrementally over the holding tube until the target F_0 value was reached. While a target F_0 value greater than 3.0 is common (Parrott 1992; Ramaswamy and others 1997), we selected a value of 6.0 to account for potential process fluctuations. Thereafter, computation was terminated, and the holding tube length calculated and specified. The program flowchart is shown in Figure 5 A and B.

Thermal and electrical verification

The model was subjected to thermal and electrical verification experiments to determine if fluid temperatures and current draw predictions were accurate. The ohmic system was presterilized with sodium sulfate solution. Product was prepared by adding marinated chicken and blanched vegetables to the mixing tank containing chow mein sauce, mixing and heating until the starch gelatinized. The product was maintained at 81.0 °C in the tank for 15 min before processing to ensure that the temperatures of solid pieces and sauce had equilibrated. The product was then pumped through the system with volumetric flow rate of 1.0×10^{-4} m^3/s, and fluid temperatures were monitored at heater inlet, heater outlet, and holding tube outlet. In addition, voltage and current were monitored within each heater. Model predictions were compared to experimental data.

Microbiological validation

Microbiological validation tests were conducted at two processing levels based on the results from the mathematical model: one a target process (139.6 °C corresponding to sterility) and one under target (117.9 °C; less than sterile).

In pilot plant trials, product was prepared as described above, and processing began. Once steady operation was achieved, 600 inoculated particles were mixed with the product in the tank, processed, recovered, and aseptically collected within a HEPA-filtered laminar flow hood. A total of 300 inoculated particles were recovered and transferred into a sterilized stomacher bag (20 particles in each bag) for incubation. Details of processing and microbiological protocols are provided by Kamonpatana and others (2013).

Statistical considerations and analysis

a. Model accuracy was verified by using a one-sample t-test with 95% confidence. Properties and temperature data were subjected to analysis of variance (ANOVA). Regression analysis was used for the microbial kinetic study, using MINITAB (v. 16, Minitab Inc., State College, Pa., U.S.A.).

b. The mean absolute error (MAE) (Lewis 1982) given below was used to compare predicted with experimental temperature of the liquid phase:

$$MAE = \frac{1}{n}\sum_{t=1}^{n}|e_t| \tag{36}$$

$$e_t = X_t - Y_t \tag{37}$$

c. The mean absolute percent error (MAPE) given below was also used to compare simulated with actual input current:

$$MAPE = \frac{1}{n}\sum_{t=1}^{n}\left|\frac{e_t}{Y_t}\right| \tag{38}$$

MAPE < 10% indicated a very accurate estimation (Lewis 1982).

d. For the RTD and microbiological studies, it is necessary to sample outliers from the population with a high degree of reliability. To achieve 95% confidence (C) of measuring the fastest first

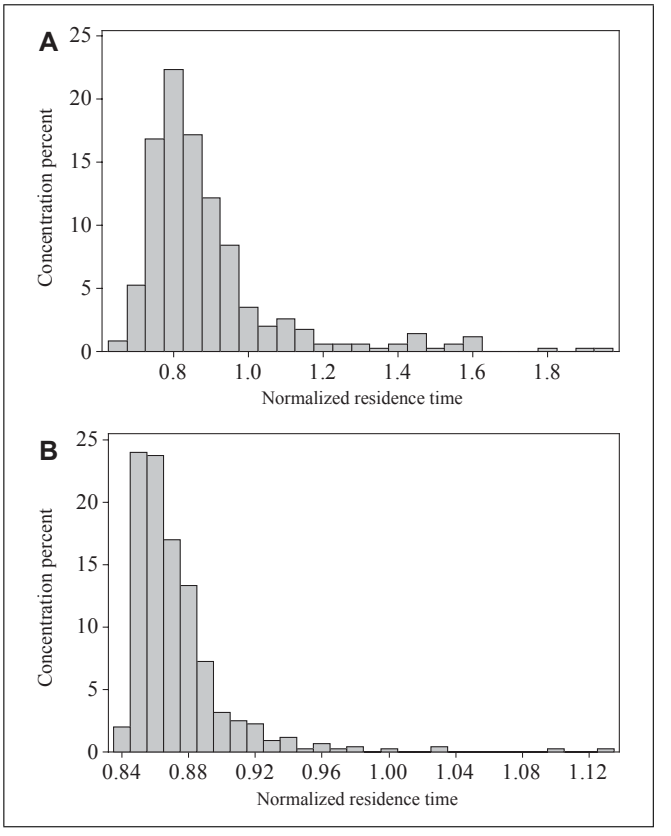

Figure 8–Density function $E(\theta)$ of the normalized particle residence time in (A) the ohmic heater and (B) holding section.

percentile (P) of the population, a minimum of 299 particles (N) must be tested, based on the following equation of nonparametric statistics (Digeronimo and others 1997):

$$N = \frac{\log(1 - C)}{\log(1 - P)} \quad (39)$$

Results and Discussion

Food properties

Properties of chicken chow mein components and chicken-alginate particles used in the mathematical model are presented in Table 3. Thermal diffusivity of chicken pieces was lower than that of other chicken chow mein components; and diffusivity of chicken-alginate particles was lower than that of the chicken pieces, verifying the conservative nature of our experimental design. Density of chicken pieces and chicken-alginate particles with and without RFID tags were not significantly different ($P > 0.05$) (Table 3), as is necessary if RTDs of the two samples were to be the same. Figure 6 shows that electrical conductivity of chow mein sauce was far higher than that of other chicken chow mein components; and the electrical conductivity of marinated chicken pieces was higher than that of chicken-alginate particles ($P < 0.05$).

Kinetic parameters of *C. sporogenes*

Survivor curves at different treatment temperature compared with heating time for *C. sporogenes* PA 3679 in chicken-alginate puree are shown in Figure 7A, and the thermal death time curve is shown in Figure 7B. The kinetic data are summarized in Table 4. The *Z*-value for *C. sporogenes* PA 3679 was calculated as 10.0 °C, which is comparable to the accepted *Z*-value of *C. botulinum*; thus, *C. sporogenes* PA 3679 may be considered an appropriate marker organism in this case.

RTD

Table 5 shows that the MNPRT was 0.64 in the heating section and 0.84 in the holding tube, thereby indicating that the velocity of the fastest particle was 1.56 and 1.19 times the average bulk velocity in the heater and holding sections, respectively. These values indicated that the worst case were well within the normally accepted conservative value of 2 for laminar flow in a tube (Alhamdan and Sastry 1997; Awuah and Simpson 1997; Sastry 1997).

The mean normalized particle residence time of heating and holding sections was equal to 0.89 and 0.87, respectively, which implied that the velocity of the average particle was higher than that of the bulk product. The flow behavior of solid pieces suspended in chow mein sauce of the heater and holding tube is presented in Figure 8. The RTD curve in the holding tube was narrower than that of the ohmic heaters. Sandeep and others (1999) suggested that the development of secondary flow caused by bends in the holding tube accounted for the narrowing of the particle residence time. Overall, the results suggest a flow that is close to plug flow, with some outlier particles in each case. In the heaters, the outliers are mostly slower than the mean residence time, with a few particles moving faster than the mean. This suggests that the general modeling approach is realistic, in that we have a largely plug-flow with some outliers.

Thermal and electrical verification and temperature distribution

Table 6 illustrates the comparison between model predictions and experimental results. The predicted and experimental fluid temperatures at heater and holding tube outlet were in good agreement with the maximum of the MAE being 0.6 °C. Comparison between simulated and actual current showed that the MAPE was no more than 7.08% at target treatment and 3.76% at the below target treatment. This indicates that the model performs well both for thermal and electrical prediction using separate and independent measures.

The heating pattern of chow mein sauce at the target and below target F_0 treatments is presented in Figure 9. The temperature of the sauce dramatically increased when the product passed through the first, second, and third heater. The discontinuity of the curve occurred due to the absence of electric field within the connecting and holding tubes. This phenomenon was observed by Sastry (1992) and Chen and others (2010). The graph also shows that fluid temperature from simulation was not significantly different from that from experiments at the heater and holding tube outlet ($P > 0.05$).

Based on the data of MNPRT from the RTD study coupled with fluid temperature data in Figure 9, the cold-spot temperatures of the fastest-moving particle of bean sprout, celery, water chestnut, mushroom, chicken piece, and chicken-alginate particle were calculated and shown in Figure 10. As expected from their thermal and electrical properties, the chicken piece was determined as the slowest-heating particle among the solid food components due to its large size, low electrical conductivity, and low thermal diffusivity. Our surrogate chicken-alginate particle heated slower than the chicken pieces, and therefore is appropriate as the worst-case particle for a microbiological validation test.

The simulation showed that cold spot of the chicken-alginate particle was located in the center. To achieve a specific target lethality at the center of the slowest heating of chicken-alginate particles, the required holding tube length was 22 m at the target (139.6 °C) process temperature (Figure 11). As expected, at 117.9 °C process temperature, the slowest-heating particle did not achieve the target lethality with the specified holding tube length. Based on the above simulations, a 22 m length holding tube was assembled and used for thermal/electrical verification and microbiological validation.

Microbiological validation of the model

The results from the inoculated pack studies are summarized in Table 7. The treatment at target temperature of 139.6 °C with 22 m holding tube length was adequate for inactivating 5 logs of *C. sporogenes* PA 3679 spores, with surviving spore counts being below the detection limit of 1 log CFU/g. These results confirmed that sterilization was achieved. Also, for the below target treatment at 117.9 °C, the inoculated pack study indicated the presence of viable microorganisms, confirming that the product was underprocessed. Thus, there was good agreement between the calculated and the experimental lethal effect. The use of a conservative model, satisfactory thermal, and electrical verification, and finally, microbiological validation show that the model is capable of designing an ohmic heating sterilization process for a multicomponent mixture.

In summary, we present an approach to determining the holding tube length for a multicomponent mixture with electric

Table 6–Comparison between model predictions and experimental results with 1.6 gpm (1.0×10^{-4} m^3/s) volumetric flow rate.

		Temperature at heating outlet (°C)	Temperature at holding tube outlet (°C)	Voltage at the 1st heater (V)	Voltage at the 2nd heater (V)	Voltage at the 3rd heater (V)	Current at the 1st heater (A)	Current at the 2nd heater (A)	Current at the 3rd heater (A)
Target	Program	139.5[a]	126.7[a]	117	117	117	72.22	62.13	55.46
	Actual (average)	139.6[a]	126.1[a]	117	117	117	77.49	65.39	57.54
	MAE	**0.1**	**0.6**	–	–	–	–	–	–
	MAPE	–	–	–	–	–	**7.08%**	**5.01%**	**3.91%**
Under target	Program	117.7[b]	107.7[b]	99	99	99	56.38	46.17	39.73
	Actual (average)	117.9[b]	107.7[b]	99	99	99	56.98	45.45	38.60
	MAE	**0.2**	**0.0**	–	–	–	–	–	–
	MAPE	–	–	–	–	–	**2.51%**	**3.32%**	**3.76%**

[a,b]Mean values of temperature sharing the same superscript are not significantly different ($P > 0.05$).
–Not applicable.

field parallel to the flow. Based on our previously published information (in particular, Salengke and Sastry 2007a, b) the worst case corresponds to a particle with extreme difference between it and its immediate surroundings. This provides a basis for process evaluation for multicomponent mixtures, and is more complex than and distinct from the approach used in our previous work with a simple two-component system (Kamonpatana and others 2013).

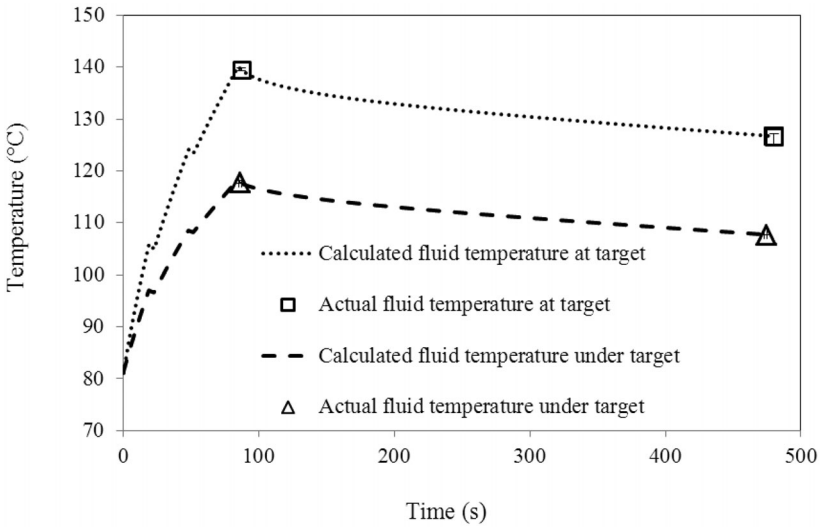

Figure 9–Comparison of predicted and experimental temperatures of carrier fluid within ohmic heaters and holding tube (target treatment: 139.6 °C and under target: 117.9 °C at heater outlet). Vertical bars represent 95% confidence interval of experimental data. The discontinuity of the curve arises from the absence of electric field when the product passes through the connecting and holding tubes.

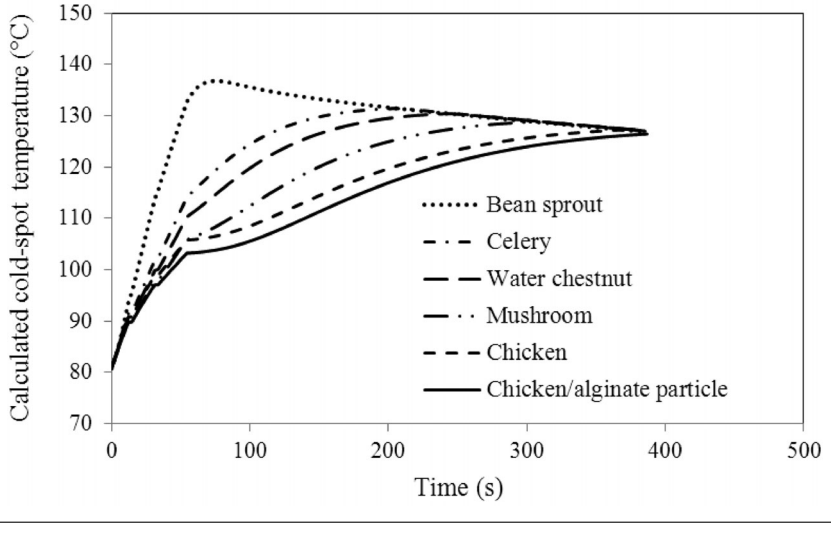

Figure 10–Calculated cold-spot temperature for the fastest-moving particles of bean sprout, celery, water chestnut, mushroom, chicken, and chicken-alginate particle at target under the worst-case scenario.

Table 7–Inoculated pack study results of chicken-alginate particles inoculated with *C. sporogenes* PA 3679 spores.

Inoculated levels	Number of particles	Process levels	Fluid temperature at heating outlet	Fluid temperature at holding tube outlet	Calculated F_0 at cold spot of the slowest-heating particle	Microbiological validation test
CFU/g			°C	°C	minute	
5.6×10^5	300	Target	139.6	126.1	6	Negative
5.6×10^5	300	Under target	117.9	107.7	<1	Positive

Conclusions

A mathematical model has been developed for ohmic heating of a liquid food containing five different types of solid food particles in a continuous flow ohmic heating system where the electric field is aligned parallel to the product flow. Among other solid components, chicken piece was found to be the slowest-heating particle from the worst-case simulation. The mathematical model was validated thermally and electrically, by comparing simulated with experimental fluid temperatures and current, as well as microbiologically with over 299 inoculated alginate particles. The predicted and experimental fluid temperatures as well as current were in good agreement. Results from microbiological tests indicated no-growth at a target F_0 treatment and positive growth at the below-target treatment, in agreement with predictions. These findings demonstrate that a mathematical modeling and microbiological verification strategy exists to help ensure sterility in a continuous flow ohmic sterilization process for a multicomponent mixture.

Acknowledgments

The authors gratefully acknowledge the financial and research support provided in part by USDA National Integrated Food Safety Initiative Project No. 2003-51110-02093; and the Ohio Agricultural Research and Development Center (OARDC), The Ohio State Univ. Simulations were achievable due to support from the Ohio Supercomputer Center Grant No. PAS0587. References to commercial products and trade names are made with the understanding that no endorsement or discrimination from the Ohio State Univ. is implied. The authors also thank Dr. Suzanne A. Kulshrestha for her help in preparation of the manuscript, and the US Army Natick Soldier Center for assistance with formulation of the test product. The authors declare that there are no conflicts of interest in this work.

Nomenclature

a = Specific surface area of particle = surface area of particle/total mixture volume
a_w = Specific surface area of wall = surface area of wall/volume
A = Area
Acs = Area of cross section
A_w = Wall surface area: for an incremental section = $\pi D \Delta x$
C = Confidence level
C_p = Specific heat
D = Diameter of heater and tube
d = Diameter of agitator shaft
F_0 = Lethality
h_{fp} = Fluid to particle convection heat transfer coefficient
h = Heat transfer coefficient
I = Current
k = Thermal conductivity
m = Temperature coefficient of electrical conductivity
$\dot{m}$ = Mass flow rate
n = Number of particles
n = Number of experimental or predicted values
$\vec{n}$ = Unit normal vector
N = Number of time steps
P = Percentage
R = Resistance
S.D. = Standard deviation
t = Time
t_h = Time at holding tube outlet
t_m = Product mean residence time
T = Temperature
U = Overall heat transfer coefficient between product and external environment
$\dot{u}$ = Rate of energy generation
V = Volume

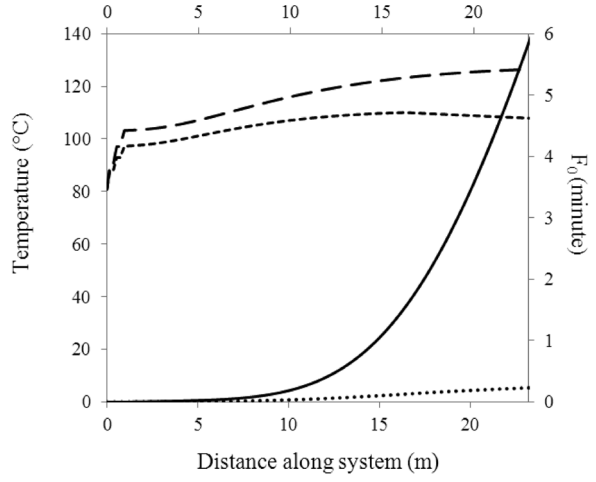

Figure 11–Cold-spot temperature and lethality of chicken-alginate particle at target value of F_0 and below target value of F_0 under the worst-case scenario.

V = Voltage
v = Volume
X = Predicted value
Δx = Incremental section thickness
Y = Experimental value
Z = Z-value

Greek Letters and Other Symbols

Δ = Increment
ρ = Density
σ = Electrical conductivity
φ = Volume fraction
∇ = Gradient

Subscripts and Superscripts

0 = Reference value for electrical conductivity
a = Ambient air
bn = Bean sprout
c = Cold spot
chk = Chicken
chn = Water chestnut
clr = Celery
f = Fluid
h = Holding tube
i = Index denoting particle type
l = Liquid
m = Mean value
m = Solid phase index
mr = Mushroom
n = Time step
p = Particle
P = Parallel
ref = Reference
s = Solid
S = Series
t = Time
w = Wall

References

Alhamdan AM, Sastry SK. 1997. Residence time distribution of food and simulated particles in a holding tube. J Food Eng 34(3):271–92.

Astrom A, Bark G. 1994. Heat transfer between fluid particles in aseptic processing. J Food Eng 21:97–125.

Awuah GB, Simpson BK. 1997. Heat transfer and lethality considerations in aseptic processing of liquid/particle mixtures: a review. Crit Rev Food Sci Nutr 37(3):253–86.

Balasubramaniam VM, Sastry SK. 1994. Liquid-to-particle convective heat transfer in non-Newtonian carrier medium during continuous tube flow. J Food Eng 23(2):169–87.

Brown KL, Ayres CA, Gaze JE, Newman ME. 1984. Thermal destruction of bacterial spores immobilized in food/alginate particles. Food Microbiol 1:187–98.

Cacace D, Palmieri L, Pirone G, Dipollina G, Masi P, Cavella S. 1994. Biological validation of mathematical modeling of the thermal processing of particulate foods: the influence of heat transfer coefficient determination. J Food Eng 23(1):51–68.

Chen C, Abdelrahim K, Beckerich I. 2010. Sensitivity analysis of continuous ohmic heating process for multiphase foods. J Food Eng 98(2):257–65.

De Alwis AAP, Fryer PJ. 1990. A finite-element analysis of heat generation and transfer during ohmic heating of food. Chem Eng Sci 45(6):1547–59.

Digeronimo M, Garthright W, Larkin J. 1997. Statistical design and analysis. Food Technol 51(10):52–6.

Fryer PJ, de Alwis AAP, Koury E, Stapley A, Zhang L. 1993. Ohmic processing of solid-liquid mixtures: heat generation and convection effects. J Food Eng 18(2):101–25.

Gaze EJ, Brown GD. 1990. Application of alginate particle techniques for the assessment of lethality in UHT processes. J Soc Dairy Technol 43(2):49–52.

Kamonpatana P, Mohamed H, Shynkaryk M, Heskitt BF, Yousef AE, Sastry SK. 2013. Mathematical modeling and microbiological verification of ohmic heating of a solid-liquid mixture in a continuous flow ohmic heater system with electric field perpendicular to flow. J Food Eng 118(3):312–25.

King A, Kaletunc G. 2009. Retrogradation characteristics of high hydrostatic pressure processed corn and wheat starch. J Therm Anal Calorim 98(1):83–9.

Lewis CD. 1982. Industrial and business forecasting methods: a practical guide to exponential smoothing and curve fitting. London: Butterworth Scientific. p 39–40.

Marcy J. 1997. Biological validation. Food Technol 51(10):48–52.

Naim F, Zareifard MR, Zhu S, Huizing RH, Grabowski S, Marcotte M. 2008. Combined effects of heat, nisin and acidification on the inactivation of *Clostridium sporogenes* spores in carrot-alginate particles: from kinetics to process validation. Food Microbiol 25(7):936–41.

Orangi S, Sastry S, Li Q. 1998. A numerical investigation of electroconductive heating in solid-liquid mixtures. Intl J Heat Mass Transf 41(14):2211–20.

Palaniappan S, Sastry S. 1991. Modelling of electrical conductivity of liquid-particle mixtures. Trans IChemE C 69:167–74.

Parrott DL. 1992. Use of ohmic heating for aseptic processing of food particulates. Food Technol 45:68–72.

Rajan S, Pandrangi S, Balasubramaniam VM, Yousef AE. 2006. Inactivation of *Bacillus stearothermophilus* spores in egg patties by pressure-assisted thermal processing. LWT Food Sci Technol 39(8):844–51.

Ramaswamy H, Awuah G, Simpson B. 1997. Heat transfer and lethality considerations in aseptic processing of liquid/particle mixtures: a review. Crit Rev Food Sci Nutr 37(3):253–86.

Ranz WE, Marshall WR Jr. 1952. Evaporation from drop. Chem Eng Prog 48(4):141–6.

Salengke S, Sastry SK. 2007a. Experimental investigation of ohmic heating of solid-liquid mixtures under worst-case heating scenarios. J Food Eng 83:324–36.

Salengke S, Sastry SK. 2007b. Models for ohmic heating of solid-liquid mixtures under worst-case heating scenarios. J Food Eng 83:337–55.

Sandeep KP, Zuritz CA, Puri VM. 1999. Determination of lethality during aseptic processing of particulate foods. Food Bioprod Process 77(1):11–7.

Sarang S, Heskitt B, Tulsiyan P, Sastry SK. 2009. Residence time distribution (RTD) of particulate foods in a continuous flow pilot-scale ohmic heater. J Food Sci 74(6):E322–7.

Sarang S, Sastry SK, Gaines J, Yang TCS, Dunne P. 2007. Product formulation for ohmic heating: blanching as a pretreatment method to improve uniformity in heating of solid-liquid food mixtures. J Food Sci 72(5):E227–34.

Sarang S, Sastry SK, Knipe L. 2008. Electrical conductivity of fruit and meats during ohmic heating. J Food Eng 87:351–6.

Sastry SK. 1992. A model for heating of liquid-particle mixtures in a continuous flow ohmic heater. J Food Process Eng 15:263–78.

Sastry SK. 1997. Measuring the residence time and modeling a multiphase aseptic system. Food Technol 51(10):44–8.

Sastry SK. 2008. Ohmic heating and moderate electric field processing. Food Sci Technol Intl 14(5):419–22.

Sastry SK, Cornelius BD. 2002. Aseptic processing of foods containing solid particulates. New York: John Wiley and Sons, Inc. 247 p.

Sastry SK, Li Q. 1996. Modeling the ohmic heating of foods. Food Technol 50(5):246–8.

Sastry SK, Palaniappan S. 1992a. Mathematical modeling and experimental studies on ohmic heating of liquid-particle mixtures in a static heater. J Food Process Eng 15:241–61.

Sastry SK, Palaniappan S. 1992b. Ohmic heating of liquid-particle mixtures. Food Technol 46(12):64–7.

Sastry SK, Salengke S. 1998. Ohmic heating of solid-liquid mixtures: a comparison of mathematical models under worst-case heating conditions. J Food Process Eng 21:441–58.

Singh RP, Heldman DR. 2001. Introduction to food engineering. 3rd ed. California: Academic Press. p 219–22.

Shynkaryk M, Sastry SK. 2012. Simulation and optimization of the ohmic processing of highly viscous food product in chambers with sidewise parallel electrodes. J Food Eng 110(3):448–56.

Tulsiyan P, Sarang S, Sastry SK. 2009. Measurement of residence time distribution of a multi-component system inside an ohmic heater using radio frequency identification. J Food Eng 93(3):313–7.

U.S. Department of Agriculture, Agricultural Research Service (USDA). 2011. USDA Nutrient Database for Standard Reference, Release 24. Nutrient Data Laboratory Home Page. Available from: http://www.ars.usda.gov/ba/bhnrc/ndl. Accessed 2012 Feb 19.

Zaror C, Pyle D, Molnar G. 1993. Mathematical modelling of an ohmic heating steriliser. J Food Eng 19(1):33–53.

Zitoun K, Sastry S, Guezennec Y. 2001. Investigation of three dimensional interstitial velocity, solids motion, and orientation in solid-liquid flow using particle tracking velocimetry. Intl J Multiphas 27(8):1397–414.

Zoltai P, Swearingen P. 1996. Product development considerations for ohmic processing. Food Technol 50(5):263–6.